Research Article

INTERNATIONAL JOURNAL OF ADVANCED ROBOTIC SYSTEMS

International Journal of Advanced Robotic Systems
January-February 2017: 1–12

DOI: 10.1177/1729881416678141
journals.sagepub.com/home/arx
SAGE

Control and flight test of a tilt-rotor unmanned aerial vehicle

Chao Chen, Jiyang Zhang, Daibing Zhang and Lincheng Shen

Abstract

Tilt-rotor unmanned aerial vehicles have attracted increasing attention due to their ability to perform vertical take-off and landing and their high-speed cruising abilities, thereby presenting broad application prospects. Considering portability and applications in tasks characterized by constrained or small scope areas, this article presents a compact tricopter configuration tilt-rotor unmanned aerial vehicle with full modes of flight from the rotor mode to the fixed-wing mode and vice versa. The unique multiple modes make the tilt-rotor unmanned aerial vehicle a multi-input multi-output, non-affine, multi-channel cross coupling, and nonlinear system. Considering these characteristics, a control allocation method is designed to make the controller adaptive to the full modes of flight. To reduce the cost, the accurate dynamic model of the tilt-rotor unmanned aerial vehicle is not obtained, so a full-mode flight strategy is designed in view of this situation. An autonomous flight test was conducted, and the results indicate the satisfactory performance of the control allocation method and flight strategy.

Keywords

Tilt-rotor UAV, control allocation, flight strategy, flight test, tricopter configuration

Date received: 1 August 2016; accepted: 9 October 2016

Topic: Special Issue - Intelligent Flight Control for Unmanned Aerial Vehicles
Topic Editor: Mou Chen

Introduction

Vertical take-off and landing unmanned aerial vehicles (VTOL UAVs) have become a focus of UAV research. Compared with rotor UAVs, VTOL UAVs can be used in scenarios that require higher speeds, longer flight ranges, or larger payload capacities. Compared with fixed-wing UAVs, VTOL UAVs could be used without the need of runway which extend application domain. Considered to be a promising VTOL configuration, the tiltrotor UAV is actively researched in the field of academics and industry due to the controllability and stability in vertical flight.[1] Some large-scale examples of such tilt-rotor UAVs include the Bell Eagle Eye,[2] SMART UAV[3] developed by the Korea Aerospace Research Institute, and the IAI Panther.[4] Moreover, many smaller scale tilt-rotor UAVs have been developed, including FireFLY6,[5] Orange Hawk,[6] TURAC,[7] and TRON[8] shown in Figure 1.

Aiming at the applications in tasks characterized by constrained or small scope areas such as power line inspection, urban traffic supervision, earthquake disaster area reconnaissance, and express delivery in mountainous regions, this article proposes a compact electrically powered tilt-rotor UAV, the main parameters of which are listed in Table 1. The tilt-rotor UAV adopts a tricopter configuration and compared with the dual propeller configuration, which requires cyclic control, the tricopter configuration reduces the mechanical complexity and control difficulty. Compared with other multi-rotor configurations, the number of actuators is reduced, which means lower cost, increased energy

College of Mechatronics and Automation, National University of Defense Technology, Changsha, Hunan, China

Corresponding author:
Chao Chen, National University of Defense Technology, Changsha, Hunan 410073, China.
Email: xueyingmo@163.com

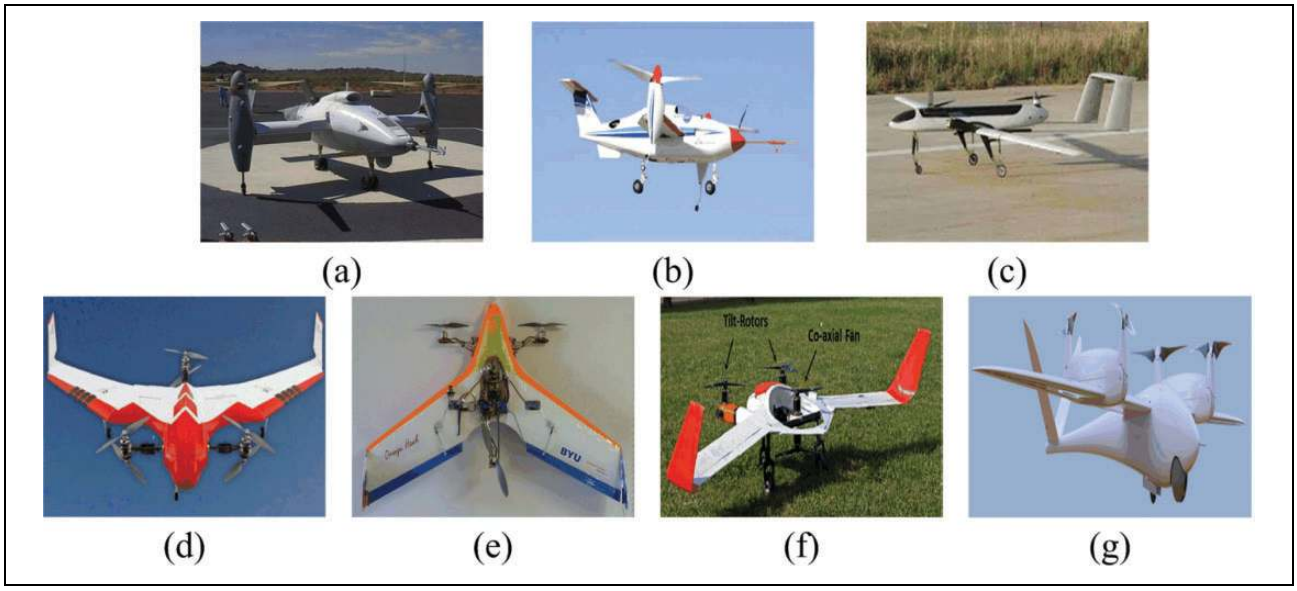

Figure 1. Examples of tiltrotor UAVs. (a) Bell Eagle Eye, (b) SMART UAV, (c) Panther, (d) FireFLY6, (e) Orange Hawk, (f) TURAC, and (g) TRON. UAVs: unmanned aerial vehicles.

Table 1. Specifications of the tilt-rotor UAV.

Specifications	Value
Flight time	40 min
Maximum flight altitude	>1 km
Weight	3.33 kg
Wingspan	1.7 m
Length	0.96 m
Cruise speed	18 ms^{-1}

UAVs: unmanned aerial vehicles.

savings, and longer flight durations. There are several unique features in the structural design that distinguishes this work from other tricopter UAVs found in the literature. In the tricopter configuration, the yaw moment that causes unstable motion induced by the reaction torque from the unpaired rotors is resolved using a rear coaxial rotor, as in TURAC and using all three coaxial rotors as in FireFLY6. However, both configurations increase the number of rotors, which will eliminate the advantage of the tricopter configuration compared with the multi-rotor configuration. The tilt-rotor UAV proposed in this work balances the yaw moment via the differential tilting of the front rotors, as in IAI Panther[4] that does not increase the number of actuators. Compared with mini IAI Panther[4] and IAI Panther, the proposed tilt-rotor UAV is a more compact and light-weight platform, which ensures that it is man-portable, with a wingspan of 1.7 m versus wingspans of 3.5 and 8 m and a weight of 3.33 kg versus weights of 12 and 65 kg.

The ability to realize multi-mode flight brings about many benefits; however, it also poses certain challenges for the problem of control. The actuators and control logic in different flight modes are different, the control weights of the rotor and fixed-wing modes need to be distributed based on efficiency, and control must be allocated to different actuators based on the control logic during the transition process. The thrust vector varies during the transition process, leading to a non-affine system and introducing dramatic cross coupling effects between the pitch, roll, yaw, and thrust channels. This is in contrast to ordinary fixed-wing UAVs, which can decouple the vertical and lateral channels. Moreover, the induced airflow varies due to tilting during the transition, aggravating the system nonlinearity and uncertainty of the mode. These features make it difficult to build an accurate mathematical model.

Considering these challenges, many scholars have conducted numerous related studies in the simulation environment. Rysdyk and Calise[9] applied a neural network (NN)-augmented model inversion control to the longitudinal channel of the generic tilt-rotor simulator; however, the control characteristics of the transition flight were not discussed. Kang et al.[10] took 40% scale smart UAV model as an object and designed an NN adaptive controller for the outer speed loop and the inner attitude loop. The simulation results of the autonomous waypoint guidance showed that the UAV could fly in the full flight envelope, including automatic conversion and reconversion under turbulent wind conditions. Kim et al.[11] adopted dynamic inversion applied to both inner loop stability and control augmentation system (SCAS) and an outer loop trajectory tracking system based on the time scale separation approach. The simulation verified the stability of the hovering mode and performance of the trajectory tracking from the fixed-wing mode to the rotor mode without full-mode flight. Chowdhury et al.[12] designed a backstepping-based proportional-derivative (PD) controller for position and attitude control. The simulation results demonstrated

stabilization in a hovering experiment and ensured the convergence of the system in a tracking experiment; however, the dynamic mode ignored the aerodynamics of the airframe. Jin et al.[13] proposed a manipulation assignment strategy of full-mode flight by trim analysis and adopted the proportional–integral–derivative (PID) controller for each channel. The simulation showed the process of the full-mode flight had little fluctuation in attitude and velocities. Some researches are conducted in the actual flight experiment. Yuksek et al.[7] successively designed a cascade control system including angular rate feedback, attitude feedback, and speed feedback and adopted a PID controller for the roll, pitch, and yaw channels. A flight experiment demonstrated a hover to transition maneuver. Kang et al.[14–16] combined a rotor governor for a constant rotor speed and attitude SCAS feedback PID controller to ensure stability of the roll, pitch, and yaw channels as the most basic control logics. The flight experiment realized the full autonomous flight from take-off to landing by tracking a curve inside the conversion corridor. However, the establishment of the conversion corridor required an accurate model via wind tunnel testing, which is expensive. Jiandong et al.[17] designed an explicit model following control system and H ∞ loop shaping design procedure for different flight modes and adopted multi-model adaptive control to switch between different control laws. Simulations and full-mode flight test verified the effectiveness of the control method; however, the research also established the aerodynamics of the UAV and determined full-mode flight strategy based on wind tunnel testing.

As reviewed earlier, most studies are based on simulations, few studies that have evolved to flight testing adopt the PID method in full-mode flight. However, these studies rely on accurate models, which are expensive to achieve. In view of that, realizing full-mode autonomous flight without an accurate model to reduce the cost motivates this work. This work adopts a PID method for controlling the attitude as well. Moreover, considering that the number of actuators is not equal to the number of control channels in the rotor mode and transition process, direct inversion cannot be applied; in addition, the control system is not input-affine, which increases the difficulty of control allocation. This will aggravate multi-channel coupling and the control error if control allocation is not properly addressed. Many control allocation strategies have been proposed such as direct control allocation,[18] pseudo inverse,[19] a daisy chaining logic,[20] linear programming,[21] and quadratic programming.[22] Considering the feature of the proposed tilt-rotor UAV, a control allocation method that can reduce the inaccuracy of the pseudo inverse method and be less complex than linear programming or quadratic programming methods is designed to make the mixer adaptive to the full-mode flight.

The major contributions of this article are as follows: First, we construct a tricopter configuration tilt-rotor UAV prototype, which reduce the number of actuators and is more portable and compact, compared to other UAVs with the same configuration; second, we design a full-mode flight strategy realizing full-mode autonomous flight without an accurate dynamic model; and finally, we design a control allocation method to make the controller adaptive to full-mode flight better.

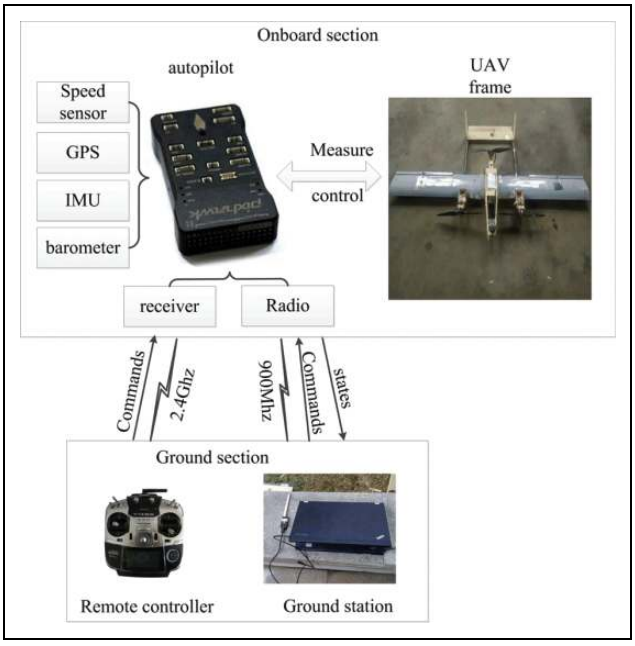

Figure 2. Block diagram of the experimental flight system.

The remainder of this article is organized as follows. The second section presents the tilt-rotor UAV prototype. In the third section, the flight control design is provided. The actual flight experiment is implemented in the fourth section. Finally, the conclusion and future work are discussed in the fifth section.

The tilt-rotor UAV platform

The partial experimental settings of the tilt-rotor UAV platform are shown in Figure 2. The platform consists of the onboard section, which includes the UAV frame and autopilot, and the ground section, which includes a ground station and a remote controller.

The autopilot can measure the flight states, send the states to the ground station, and control the flight of the UAV. The autopilot adopts the Pixhawk autopilot system made by 3DRobotics, which is an independent, open-source, open-hardware project. The Pixhawk system, running the NuttX (version 6.18) real-time operating system, utilizes a 168 MHz CortexM4FARM processor and has 256 KB of RAM and 2 MB of flash memory.[23] The system has 14 pulse-width modulation (PWM) servo outputs. The onboard sensors include an IMU, a GPS module with data updated at 5 Hz, a barometer, and a digital airspeed sensor. The UAV can be guided by both autopilot and a pilot. If the pilot finds the UAV in an abnormal flight manner, the control is switched to the remote controller

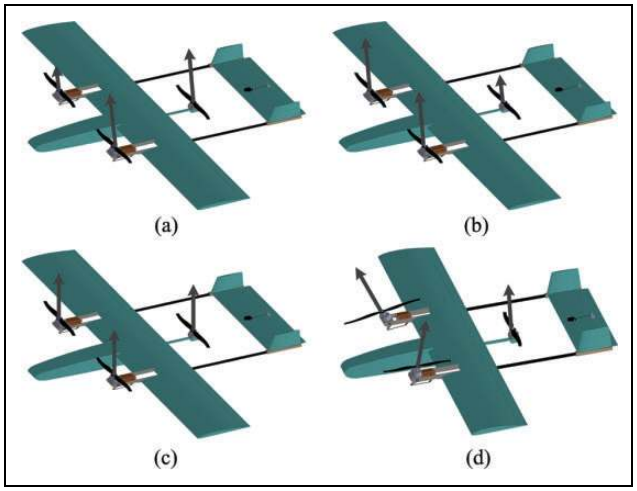

Figure 3. Control logic in rotor mode. (a) roll, (b) pitch, (c) thrust, and (d) yaw.

using a Futaba<001> T14SG 2.4 GHz transmitter to make the UAV restore safe flight. The ground station software "QGroundControl"[24] is open-source ground control software compatible with the Pixhawk autopilot. The ground station is used to observe the flight status of the UAV and configure and control the UAV by sending commands to the autopilot through the data link with a radio frequency of 900 MHz.

The proposed tilt-rotor UAV features a conventional aileron, elevator control surface configuration, three fixed-pitch rotors, and two servo motors. The two front rotors can tilt from vertical to horizontal positions with a tilting mechanism that is driven by two servo motor, as shown in Figure 3. The tail rotor is fixed at the rear of the vehicle vertically. When the front rotors are in the vertical position, the tilt-rotor UAV is in rotor mode. The control scheme of the rotor mode is shown in Figure 3. The roll is controlled via the differential thrusting of the two front rotors, and the pitch is controlled via the differential thrusting of the front and tail rotors. To balance the yaw moment induced by the reaction torque from the unpaired rotor, the yaw is controlled via the differential tilting of the front rotors.

When the front rotors are in the horizontal position, the front rotors only offer thrust along the longitudinal axis. With the tail rotor off, the tilt-rotor UAV is in the fixed-wing mode. The control scheme in the fixed-wing mode is similar to that of the conventional fixed-wing UAV. The roll channel is controlled by the aileron, the pitch channel is controlled by the elevator, the speed channel is controlled by the speed of the motors, and the yaw channel is controlled by the aileron because there is no rudder installed, considering that the rudder is not frequently used. The transition from the rotor mode to the fixed-wing mode is called the conversion mode. The transition from the fixed-wing mode to the rotor mode is called the reconversion mode. The different flight modes are shown in Figure 4.

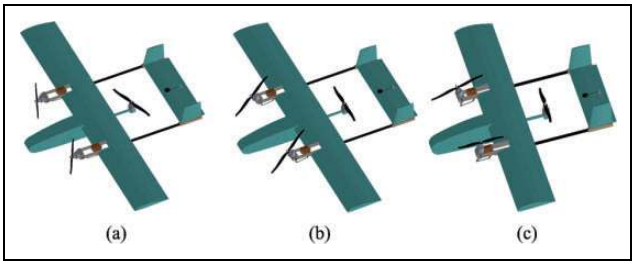

Figure 4. Different flight modes. (a) The fixed-wing mode, (b) conversion or reconversion mode, and (c) the rotor mode.

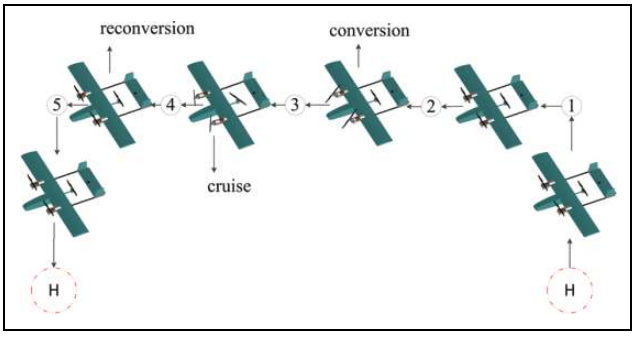

Figure 5. Flight mission profile.

If the tilting mechanisms are installed at both ends of the wing, the wing structure needs to be strengthened. To reduce the vibration of the wing caused by the tilting mechanism and to reduce the weight of the wing, the positions of the tilting mechanisms are designed to be as close as possible to the body, and the center of gravity is required to be as close as possible to the center of the triangle formed by the three rotors. The vertical and horizontal tails are of a light wood material to reduce weight, and other structures of the prototype are of a multilayer board material. The motors are T-motor MN5208. The motor–rotor couples are tested on a test bench to calculate the thrust and torque coefficient. As a result of these tests, the appropriate rotor size is chosen as 16 × 5.4 in.

Flight control system design

Full-mode flight strategy

In autonomous flight, the ground control station gives a take off command. The UAV flies along a predetermined flight path by autopilot. The switching between different flight modes is triggered by a predetermined flight point. The specific process is shown in Figure 5.

Point H is the take-off and landing point. The tilt-rotor UAV takes off in the rotor mode to maintain a stable attitude and climbs vertically at a fixed speed. After reaching the specified altitude point 1, the tilt-rotor UAV adjusts the yaw angle so that the head points to the intended direction of flight. After adjusting the direction, the tilt-rotor UAV flies toward flight point 2, and flight

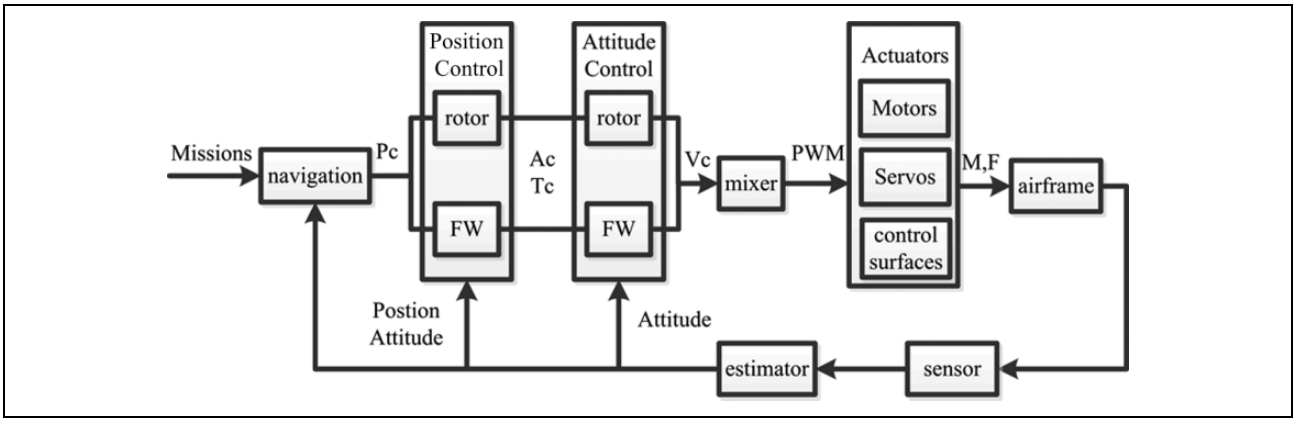

Figure 6. The control structure. P_c, A_c, and T_c represent the position, attitude, and thrust command, respectively. V_c represents the virtual control command. FW represents the fixed-wing mode. PWM: pulse-width modulation.

point 2 triggers the conversion command. The conversion mode consists of stages P1 and P2. In stage P1, the tilt-rotor makes a negative pitch angle θ to accelerate; meanwhile, the rotors begin to tilt at a fixed rate until a preset maximum tilting angle. When the switching speed is reached, the tilt-rotor UAV is into stage P2. The rotors first stop, and then, the tilt-rotor UAV instantaneously switches to the fixed-wing mode. Once in the fixed-wing mode, rotors 1 and 2 accelerate to ensure that the airspeed remains above the stall speed with a large throttle for a period of time, and rotor 3 stops running. If, in conversion mode, the UAV remains unable to accelerate to the switching speed for 5 s, the tilt-rotor UAV switches to the rotor mode and returns home. After the airspeed increases to above the stall speed, the tilt-rotor UAV flies toward point 3. When the tilt-rotor UAV reaches navigation point 4, the reconversion mode is triggered. First, the rotors stop, and then, the tilt-rotor UAV instantly switches from the fixed-wing mode to the rotor mode. Once in rotor mode, the rotors increase the force and stabilize the attitude. After the attitude is stable, the UAV flies toward point 5 and lands at point H at a constant speed.

The control architecture

The flight control system consists of many control modes such as manual control mode (MANUAL), altitude control mode (ALTCTL), position control mode (POSCTL), and mission control mode (MISSION). MANUAL, ALTCTL, and POSCTL require pilot participation for control. In MISSION, the UAV performs the programmed mission sent by the ground control station without the participation of pilots.[25] The control architecture in MISSION adopts a time scale separation principle consisting of a navigation loop, a position loop, an attitude loop, and the mixer, as shown in Figure 6. The estimator adopts an extended Kalman filter algorithm that uses rate gyroscopes, accelerometers, a compass, GPS, airspeed and barometric pressure measurements to estimate the position, velocity, and angular orientation of the UAV. The estimator sends these parameters to each loop. The navigation loop is responsible for the autonomous navigation functionality, which accepts missions and turns them into lower level navigation primitives such as the position commands and speed commands.

The position control loop takes the global position command and the current position as inputs and outputs the attitude and thrust command vector to the attitude control loop. In the fixed-wing mode, the position control loop is composed of the longitude control and the lateral control. The lateral control adopts the L_1 navigation logic,[26] which combines the current position of UAV and a reference point on the flight path at a distance L_1 to generate the lateral acceleration command a_{cmd}

$$a_{\text{cmd}} = \frac{2V_a^2}{L_1}\sin\eta \tag{1}$$

where η is the angle between the direction of airspeed V_a and the direction of the current position pointing to the reference point. Then the yaw command ψ_c could be calculated by the position command and the current position, the roll command ϕ_c could be calculated by a_{cmd}[27] in coordinated turn condition as follows

$$\phi_c = \arctan\frac{a_{\text{cmd}}}{g} \tag{2}$$

The longitude control adopts the total energy control system method consisting of the inner and outer loops. The outer loop adopts a PD controller for the airspeed and altitude channels, respectively. The outputs of the outer loop together with the airspeed derivative are first converted to energy rates, and then the inner loop adopts PI controller with energy rates generating the pitching command θ_c and thrust command F_{rotor}.

In rotor mode, the main procedures of the position control are presented, readers may refer to the work of Mellinger D and Kumar[28] for details of the entire algorithm: first, the position tracking error e along Z axis

of the geodetic frame (GF) generates the thrust F_Z along Z direction in GF

$$\begin{cases} e = z - z_c \\ F_Z = -k_p e - k_d \dot{e} - mg + m\ddot{z}_c \end{cases} \tag{3}$$

where z_c is the position tracking command along Z axis of GF, k_p and k_d are the control parameters, m is the mass of the UAV, and g is the gravity acceleration. The thrust command F_{rotor} could be calculated by F_Z through a coordinate transformation; then, the rotation matrix command from the body frame (BF) to GF, R_c could be calculated as follows

$$\begin{cases} z_{Bc} = \dfrac{F_Z}{\| F_Z \|} \\ y_{Bc} = \dfrac{z_{Bc} \times X}{\| z_{Bc} \times X \|} \\ x_{Bc} = y_{Bc} \times z_{Bc} \\ R_c = [x_{Bc}, y_{Bc}, z_{Bc}] \end{cases} \tag{4}$$

where $X = [\cos\psi_c,\ \sin\psi_c, 0]^T$; finally, after R_c is calculated, the attitude error vector e_R could be calculated with the current rotation matrix R from BF to GF as follows

$$e_R = 0.5(R_c^T R - R^T R_c)^V \tag{5}$$

where V represents the vee map which takes elements of $so(3)$ to $\mathbb{R}^3$.

The attitude loop in all flight modes adopts two control loops[25]: an angular loop and an angular rate loop. The angular loop, which is relative to the geodetic coordinate system, uses the P controller to achieve the angular rate command for every channel. Through a coordinate system transformation, the angular rate commands in BF are input to the angular rate loop, which uses the PID controller to generate virtual control commands as shown in the following equation

$$[M_x, M_y, M_z]^T = k_{Mp} e_r + k_{Md} \dot{e}_r + k_{Mi} \int e_r \, dt \tag{6}$$

where M_x, M_y, and M_z are the virtual control commands for roll, pitch, and yaw channels, respectively; e_r is the angular rate error vector; and k_{Mp}, k_{Md}, and k_{Mi} are controller parameters. M_x, M_y, M_z, and F_{rotor} together constitute the virtual control commands. The virtual control commands are the weighted sum of the outputs of the rotor and fixed-wing modes. The mixer used as the control allocation maps $[F_{\text{rotor}}, M_x,\ M_y,\ M_z]^T$ into the PWM of individual actuator. The PWMs drive the actuators generating the moment and force, which drives the tilt-rotor UAV motion. The sensors measure the states of the tilt-rotor UAV and output them to the estimator.

The control allocation

The inputs of the mixer are the virtual control commands of four channels $[F_{\text{rotor}}, M_x,\ M_y,\ M_z]^T$. The mixer is responsible for distributing $[F_{\text{rotor}}, M_x,\ M_y,\ M_z]^T$ among the available actuators. In the rotor mode, the control surfaces do not function. The actuators consist of three rotor speeds and two tilting angles. In the fixed-wing mode, the actuators consist of two rotors, ailerons, and elevators. In the conversion mode, the mixer needs to distribute the weights of the rotor and fixed-wing modes according to the efficiency and modify the mapping relationship according to the current tilting angle.

Table 2. The weights in different modes.

Flight mode	weight_r
Rotor mode	1
P1	1
P2	0
Fixed-wing mode	0
Reconversion mode	0

UAVs: unmanned aerial vehicles.

Because the virtual command $[F_{\text{rotor}}, M_x,\ M_y,\ M_z]^T$ is the weighted sum of the outputs of the rotor and fixed-wing modes, it could be expressed as follows

$$U = U_r \cdot \text{weight\_}r + U_f \cdot (1 - \text{weight\_}r) \tag{7}$$

where U_r is the virtual commands of the rotor mode, U_f is the virtual commands of the rotor mode, and weight_r is the weight of U_r. In the rotor mode, weight_r is 1, and in the fixed-wing mode, weight_r is 0. During the P1 stage of the conversion mode, because the direction of the rotor thrust varies during the conversion mode, the induced airflow can have a changing influence on the wings. Moreover, the airspeed of the UAV in stage P1 is low, and the efficiency of the aerodynamics is low; therefore, the force and moment produced by the control surfaces are comparatively small, changing, and difficult to evaluate accurately. weight_r is 1 during stage P2 of the conversion mode because the rotors all stop, and when the airspeed is above the switching speed, weight_r is 0. In reconversion mode, all the rotors stop, the weight_r is 0, and the airspeed remains large; therefore, U_f will work until the airspeed is reduced below the switching speed. The weights are listed in Table 2.

The force analysis for establishing the mapping relationship from the virtual control command U to the actuators is shown in Figure 7.

The two reference frames given in Figure 7 are BF $B(O_b, i_b, j_b, k_b)$ and GF $W(O_w, i_w, j_w, k_w)$. The origin O_b is the center of mass, i_b points out the nose of the airframe, j_b points out the right wing, and k_b points out the belly. The attitude of the vehicle in the GF is given as the attitude vector $\Theta = [\Phi,\ \theta,\ \Psi]^T$, which contains the roll, pitch, and yaw angles. The serial numbers of the rotors are defined in Figure 7. Rotors 1 and 3 rotate counterclockwise. Rotor 2 rotates clockwise. δ_1 and δ_2 are the tilting angles between the BF-aligned vertical axis and motor shafts 1 and 2, respectively. When the component of the rotor thrust along the x-axis is negative, the tilting angle is defined as

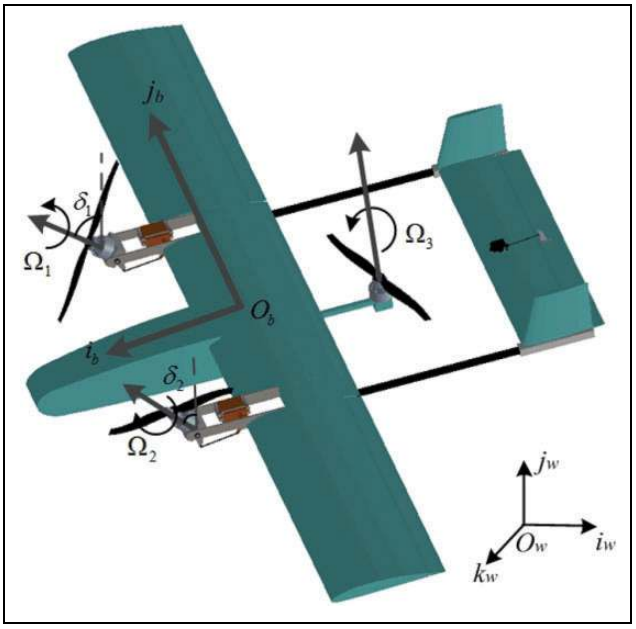

Figure 7. The body frame and geodetic frame.

negative and vice versa. The ranges of δ_1 and δ_2 are from -15° to 90°. M is the sum of all externally applied moments, defined in the BF, and the components of M are $[M_x, M_y, M_z]^T$, M could be expressed as[29]

$$M = M_{\text{gyro}} + M_{\text{rotate}} + M_{\text{thrust}} + M_{\text{aero}} \tag{8}$$

where the gyroscopic moments M_{gyro} is created by the gyroscopic effect of the motors and rotors, the reaction torque M_{rotate} is exerted on the hub of each rotor during rotation due to the drag of rotors, M_{thrust} is created by the thrusts of the rotors, and M_{aero} is created by the drag/lift forces of the wings, although this is neglecting when weight_r is 1, M_{gyro} is assumed to be insignificant compared with M_{thrust} and M_{rotate} considering that the moment of inertia of the motor is small and the tilting angular rate is low; therefore, the expressions of M_{rotate} and M_{thrust} are given as

$$M_{\text{rotate}} = k_q \left(\Omega_1^2 \begin{bmatrix} -s\delta_1 \\ 0 \\ c\delta_1 \end{bmatrix} + \Omega_2^2 \begin{bmatrix} -s\delta_2 \\ 0 \\ c\delta_2 \end{bmatrix} + \Omega_3^2 \begin{bmatrix} 0 \\ 0 \\ 1 \end{bmatrix} \right) \tag{9}$$

where s and c are short for sin and cos, respectively, k_q is the rotor moment coefficient, and Ω_1, Ω_2, and Ω_3 are the speeds of rotors 1, 2, and 3, respectively.

$$\begin{aligned} M_{\text{thrust}} = l_1 \times \begin{bmatrix} s\delta_1 \\ 0 \\ -c\delta_1 \end{bmatrix} T_1 + l_2 \times \begin{bmatrix} s\delta_2 \\ 0 \\ -c\delta_2 \end{bmatrix} T_2 \\ + l_3 \times \begin{bmatrix} 0 \\ 0 \\ -1 \end{bmatrix} T_3 \end{aligned} \tag{10}$$

where $T_i = k_t \Omega_1^2$, T_i is the thrust produced by the i th rotor, k_t is the rotor thrust coefficient, and l_i refers to the position vector from T_i to O_b, in which $l_i = l_{ix} \cdot i_b + l_{iy} \cdot j_b + l_{iz} \cdot k_b$.

F is the total external force along the Z axis in the BF based on neglecting the force generated by the aerodynamics of the airframe. The total force can be expressed as

$$F = F_g + F_{\text{rotor}} \tag{11}$$

where F_g is the gravity and F_{rotor} are the sum of thrusts of rotors. The expressions for these values are given as

$$F_{\text{rotor}} = -\cos\delta_1 T_1 - \cos\delta_2 T_2 + T_3 \tag{12}$$

$$F_g = \cos\theta \cos\phi mg \tag{13}$$

By combining formulas (9), (10), and (12), U is expressed as

$$\begin{bmatrix} M_x \\ M_y \\ M_z \\ F_{\text{rotor}} \end{bmatrix} = A \begin{bmatrix} \Omega_1^2 \\ \Omega_2^2 \\ \Omega_3^2 \end{bmatrix} \tag{14}$$

where

$$A = \begin{bmatrix} -l_{21}c\delta_1 k_t - k_q s\delta_1 & -l_{22}c\delta_2 k_t + s\delta_2 k_q & -l_{23}k_t \\ l_{11}c\delta_1 k_t + l_{31}k_t s\delta_1 & l_{12}c\delta_2 k_t + l_{32}k_t s\delta_2 & l_{13}k_t \\ -l_{21}s\delta_1 k_t + k_q c\delta_1 & -l_{22}s\delta_2 k_t - c\delta_2 k_q & k_q \\ -c\delta_1 k_t & -c\delta_2 k_t & k_t \end{bmatrix}.$$

As seen from formula (14), it is not input-affine for the actuators, and the number of actuators is greater than the number of channels. Thus, $[\Omega_1, \Omega_2, \Omega_3, \delta_1, \delta_2]^T$ cannot be solved using a pseudo inverse method. To solve this problem, the mixer divides the actuators $[\Omega_1, \Omega_2, \Omega_3]^T$ and $[\delta_1, \delta_2]^T$ into two groups and separates M_z from U considering that the yaw channel is controlled primarily by the differential tilting angle $[\delta_1, \delta_2]^T$. Therefore, at each sample, the mixer first allocates $[F, M_x, M_y]^T$ based on the current tilting angles $[\delta_1, \delta_2]^T$, and then, it allocates M_z to obtain the increments $\Delta\delta_1$ and $\Delta\delta_2$. The output of tilting angles can be obtained as follows

$$\begin{cases} \delta_1 = \delta_1 - \Delta\delta_1 \\ \delta_2 = \delta_2 + \Delta\delta_2 \end{cases} \tag{15}$$

In the first allocation, the number of actuators $[\Omega_1, \Omega_2, \Omega_3]^T$ equals the number of channels. Through inversion, the $[\Omega_1, \Omega_2, \Omega_3]^T$ can be obtained as

$$\begin{bmatrix} \Omega_1^2 \\ \Omega_2^2 \\ \Omega_3^2 \end{bmatrix} = B \begin{bmatrix} M_x \\ M_y \\ F_{\text{rotor}} \end{bmatrix} \tag{16}$$

where $B = \begin{bmatrix} -l_{21}c\delta_1 k_t - k_q s\delta_1 & -l_{22}c\delta_2 k_t + s\delta_2 k_q & -l_{23}k_t \\ l_{11}c\delta_1 k_t + l_{31}k_t s\delta_1 & l_{12}c\delta_2 k_t + l_{32}k_t s\delta_2 & l_{13}k_t \\ -c\delta_1 k_t & -c\delta_2 k_t & k_t \end{bmatrix}$

then, the yaw channel can be allocated based on the

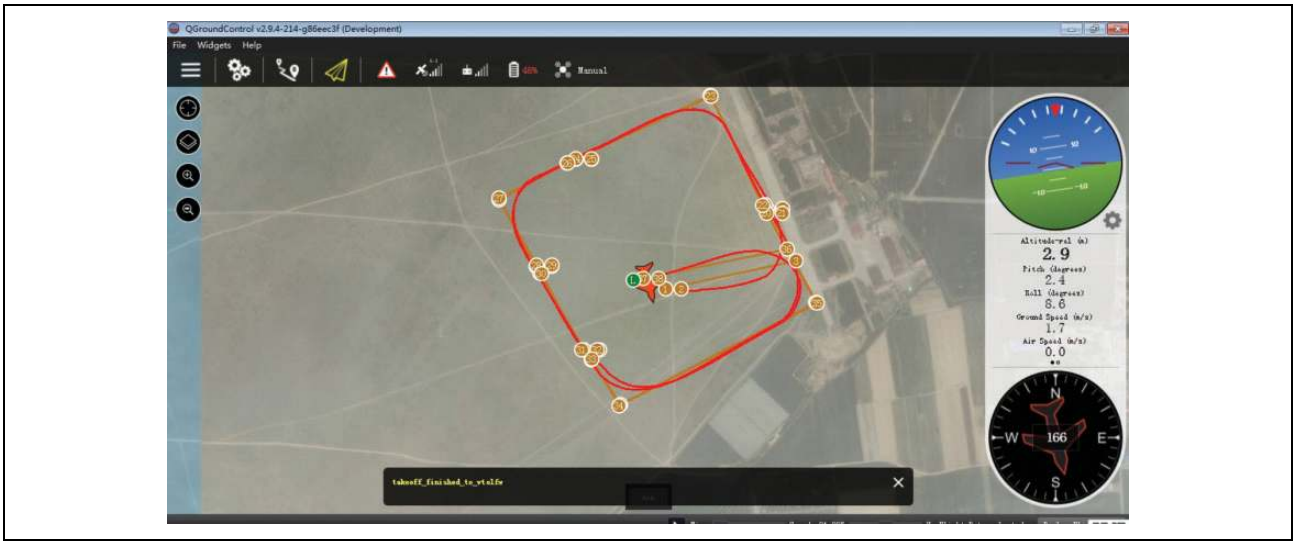

Figure 8. Flight trajectory and navigation points displayed in QGroundControl, the red line is actual trajectory, the orange is the designed trajectory.

obtained $[\Omega_1, \Omega_2, \Omega_3]^T$. When using differential tilting to balance the yaw moment, the tilt-rotor UAV makes rotors 1 and 2 tilt the same increment $\Delta\delta$ based on the current tilting angles δ_1 and δ_2 at each sample which means that $\Delta\delta_1 = -\Delta\delta_2 = \Delta\delta$. In rotor mode, δ_1 and δ_2 are small, and the efficiency of the yaw moment generated by the differential tilting angle affects obviously. The changing amplitude of $\Delta\delta$ is small when the UAV is subject to yaw motion at each sample; therefore, it will not violate the assumption that $[F_{\text{rotor}}, M_x, M_y]^T$ are allocated based on the current tilting angle. With a small-angle approximation, the $\Delta\delta$ can be obtained as follows

$$\Delta\delta = \frac{M_z + k_q\Omega_3^2 + C + D + k_q c\delta_1\Omega_1^2 - c\delta_2 k_q\Omega_2^2}{C - D - k_q s\delta_1\Omega_1^2 - s\delta_2 k_q\Omega_2^2} \quad (17)$$

where $C = l_{21}k_t\Omega_1^2 s\delta_1$, $D = l_{22}c\delta_2 k_t\Omega_2^2$. In conversion flight mode, δ_1 and δ_2 gradually increase. The efficiency of balancing the yaw moment via the differential tilting angle gradually decreases, making the $\Delta\delta$ gradually larger, which violates the assumption that $[F_{\text{rotor}}, M_x, M_y]^T$ are allocated based on the current tilting angle. Therefore, in conversion flight mode, the yaw channel will not be controlled. Although this method represents a compromise, it is feasible in actual flight considering that the duration of conversion is short. In the fixed-wing mode, the control allocation is the same as in the traditional fixed-wing mode.

Experimental results

A full-mode flight experiment including VTOL, conversion, cruising, and reconversion was implemented in the MISSION control mode with a wind speed of 2–3 ms^{-1}. The duration of the flight is less than 5 min, and the flight trajectory is preprogrammed in QGroundControl, as shown in Figure 8. The orange line is the predetermined route, and the red lines are the actual flight trajectory. The flight trajectory and the route coincide very well. The tilt-rotor UAV takes off toward navigation point 1. Point 2, which is used as a function point, shares the same physical position as point 1 for adjusting the direction and triggering the conversion command. The tilt-rotor UAV flies twice along a length of 500 m^2, and the altitude command during cruising in the fixed-wing mode is 35 m. After point 35, the tilt-rotor UAV begins to descend. Point 38 shares a physical position with point 37 for triggering the reconversion command. The tilt-rotor UAV switches to the rotor mode and lands at point L. To verify the stability and tracking performance, during cruising, the trajectory adds additional navigation points, such as points 20, 26, 30, and 33, to trigger the pitch excitations making the tilt-rotor UAV change in the pitch channel. The three-dimensional flight trajectory shown in Figure 9 is transformed from GPS records to the local frame, whose origin is the takeoff point.

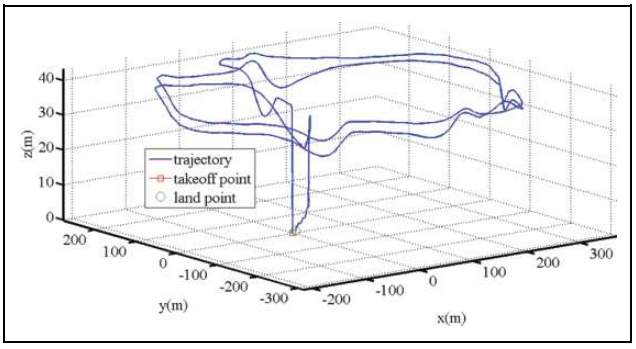

Figure 9. 3D flight trajectory during the whole flight test.

The full-mode flight mode experimental results are shown in Figure 10. Because no sensors measure the

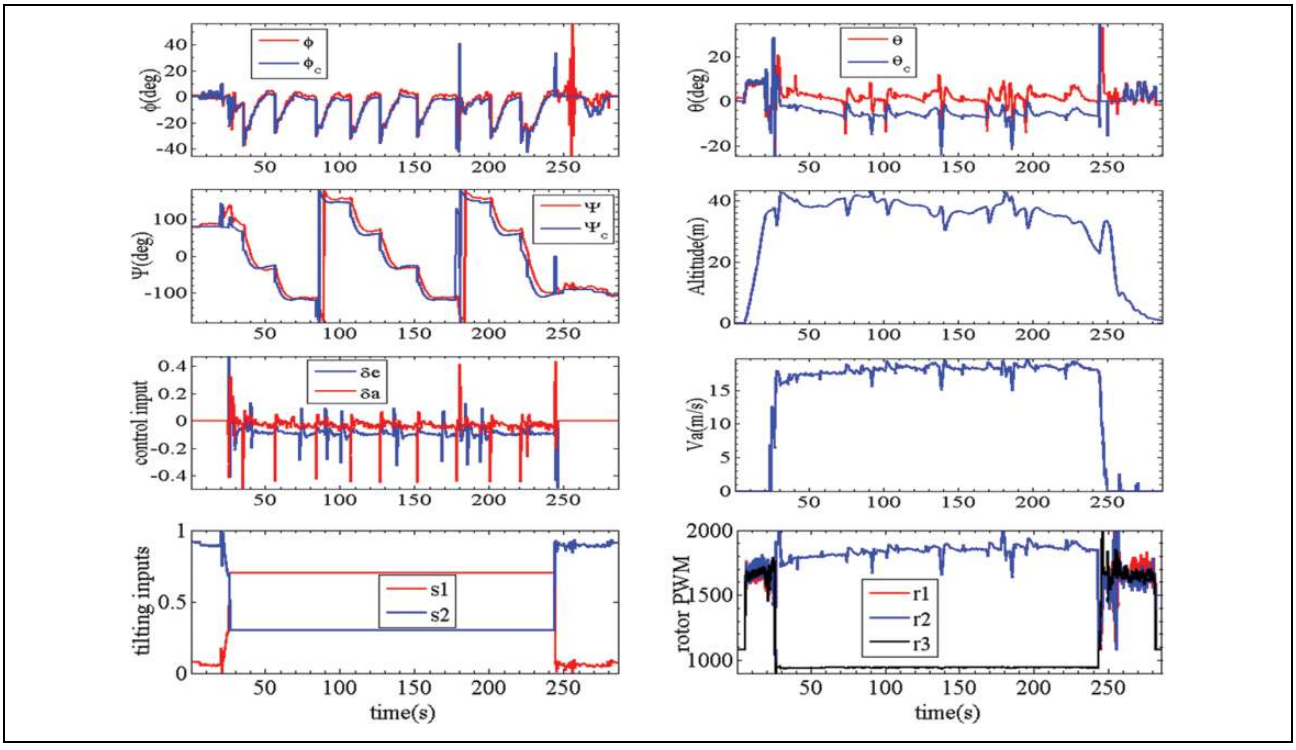

Figure 10. Flight results in full-mode flight. s1 and s2 represent the servo motors 1 and 2, respectively; r1, r2, and r3 represent rotors 1, 2, and 3, respectively.

deflection of the control surface, the normalized control inputs, which follow a linear relationship with the deflections of the corresponding control surfaces, are used to represent the deflection angles. Similarly, the tilting inputs and the PWMs of the rotors are used to represent the tilting angle of the servo motors and the speed of the rotors, respectively. The fixed-wing mode is active from 26.04 to 245 s. In the fixed-wing mode, ϕ could track the command perfectly. There is a delay in the yaw channel tracking the command. The excitations in the pitch channel are implemented by changing the control input of the elevator. The changing magnitude of the control input is 0.2 based on the current quantity. θ and the altitude oscillate with the excitations. The tilt-rotor UAV could regain trim attitude after this oscillation. θ can track the command, and the response speed is fast; however, there is an error that may be due to the use of improper controller parameters. The airspeed could ensure an airspeed command of 18 ms^{-1} when there was no excitation.

The details of the rotor and conversion flight mode are shown in Figure 11. The rotor mode is from 5.7 to 21.55 s, and the conversion mode is from 21.55 to 26.04 s. In rotor mode, ϕ and θ could track the command well; however, there was a deviation in the yaw channel that is caused by the effect of current on the compass. Although the Pixhawk was placed as far as possible away from the battery and wires, the effect on the compass cannot be eliminated. From 19.82 to 21.55 s, the tilt-rotor UAV adjusted its heading severely via differential control, the yaw response was fast, and there was no overshoot. In the conversion mode from 21.55 to 25.4 s, the roll channel remained stable, the yaw channel was not controlled, and ϕ did not track the command at all. The pitch command was gradually downward to accelerate, and θ could track the command in the first 2 s. Then, θ gradually increased without tracking the command. This phenomenon is caused by the error in the estimation of the tilting angle. Because the tilting angle is computed via the off-line calibration of the tilting input and is not achieved by the direct measurement of a sensor, the error between the actual tilting angle and the estimated angle is small when the tilting angle is small and gradually increases with increasing tilting angle. The increasing error causes the control allocation to be inaccurate, resulting in the pitch deviation. When the deviation increases, the PWM of rotor 3 increases, and the PWMs of rotors 1 and 2 decrease; in addition, θ no longer increases. Before switching to the fixed-wing mode at 25.6 s, all the rotors first stop 0.2 s prior to make the transition smooth. Once in stage P2, the control surfaces begin to take effect at 25.4 s. The switching airspeed of 12 ms^{-1} is below the stall speed; from 26.04 to 28 s, the tilt-rotor UAV applies a diving acceleration with large rotor speeds. The airspeed increases to 17 ms^{-1} at 28 s. In stage P1, the attitude is stable, and in stage P2, the attitude generates oscillations in the pitch and roll channels. The reason for this phenomenon is the switching from the rotor position control to the fixed-wing position control. However, the two channels can almost track the respective command in the conversion

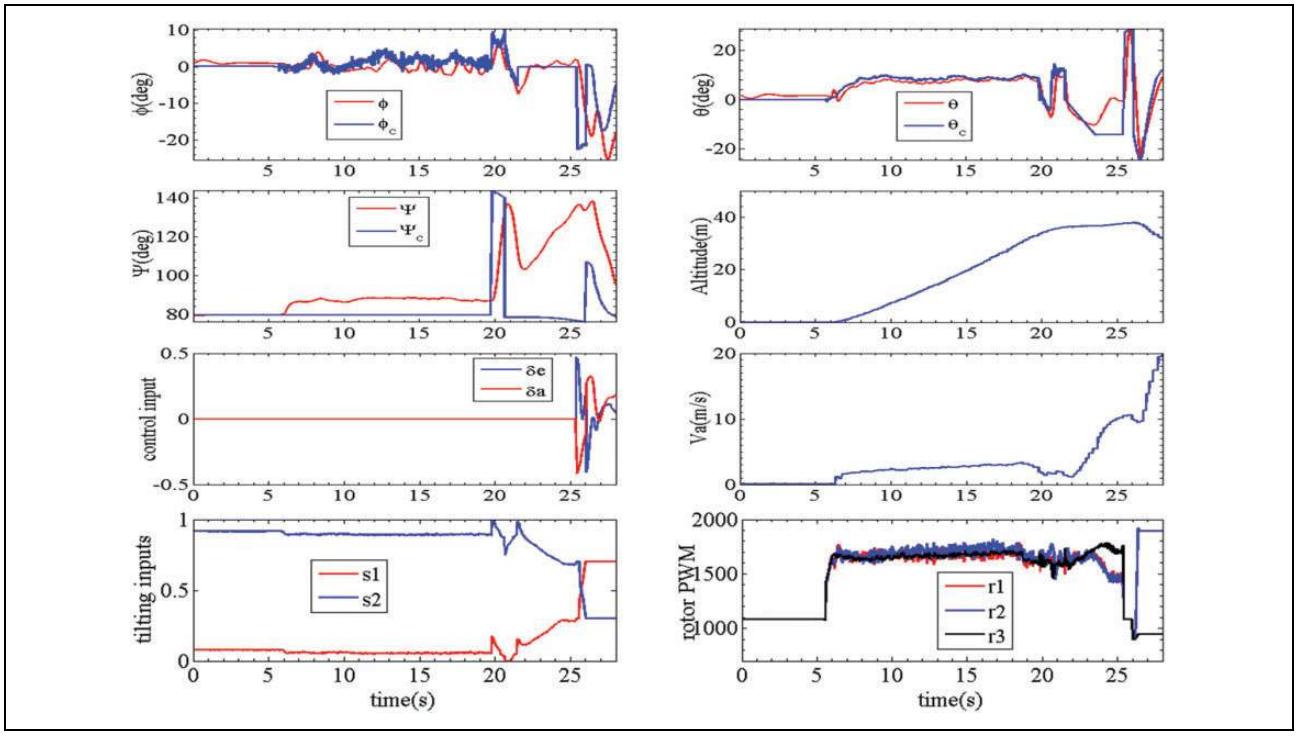

Figure 11. Flight results in rotor and conversion mode. s1 and s2 represent the servo motors 1 and 2, respectively; r1, r2, and r3 represent rotors 1, 2, and 3, respectively.

mode and converge to a steady state in the fixed-wing mode. The yaw channel generates a maximum deviation of 58° and can converge to the command in the fixed-wing mode. The altitude remains unchanged in the conversion mode and decreases by 5 m to accelerate in the fixed-wing mode.

The details of the reconversion and rotor flight mode are shown in Figure 12. The reconversion mode is from 243.1 to 243.8 s. Because the controller parameters of the fixed-wing position control and rotor position control are different, a sudden switching between two POSCTLs leads to the commands of ϕ, θ, and ψ suffering from large variations. This causes a 30° upward shift and subsequent adjustment in the pitch channel in order to track the command and slight variations in the roll and yaw channels. Although θ exhibits a large variation, the tilt-rotor UAV could restore stability within 3 s from 244 to 247 s. The altitude remained approximately constant during the reconversion mode. The control surfaces stopped having an effect until the airspeed was below the switching airspeed of 12 ms^{-1} at 246 s, which helped stabilize θ. The rotors stopped 0.3 s prior to the reconversion mode and gradually increased after the reconversion mode to make the transition smooth. In rotor mode, there were significant excursions from the stable state in the roll channel from 254 to 257 s, which may have been caused by gusts. Although the amplitude of the variation is larger than 100°, the tilt-rotor UAV was able to restore stability.

The results of the flight experiment show that, even if there is a 50° amplitude of variation in the pitch channel during the conversion mode, a series of pitching oscillations in the fixed-wing mode, a 30° amplitude of the pitch variation in the reconversion mode, and a series of roll oscillations with a magnitude of 100° in rotor mode, the tilt-rotor UAV could restore stability. This validates the performance of the mixer and the feasibility of the flight strategy. Because the reconversion mode can be achieved without deceleration, the approach distance and time are reduced. However, there is a phenomenon that need be addressed, when the tilt-rotor UAV switches between the rotor mode and the fixed-wing mode, the attitude generates a fluctuation, which may rise a difficulty in some applications that need keep continuous and stable attitude such as aerial photography. Snapshots of the flight test are presented in Figure 13.

Conclusion and future work

Aiming at portability and tasks characterized by constrained small scope areas, a tricopter configuration tilt-rotor UAV prototype is developed. The tilt-rotor UAV adopts differential tilting of the front rotors, therein reducing the number of actuators compared to other tricopter configuration tilt-rotor UAVs such as TURAC and FireFLY6. Compared to Panther and mini Panther, the proposed tilt-rotor UAV is more compact and man-portability. The controller architecture of the autonomous flight is presented. Without wind tunnel modeling a precise dynamic model, a feasible full-mode flight strategy is designed

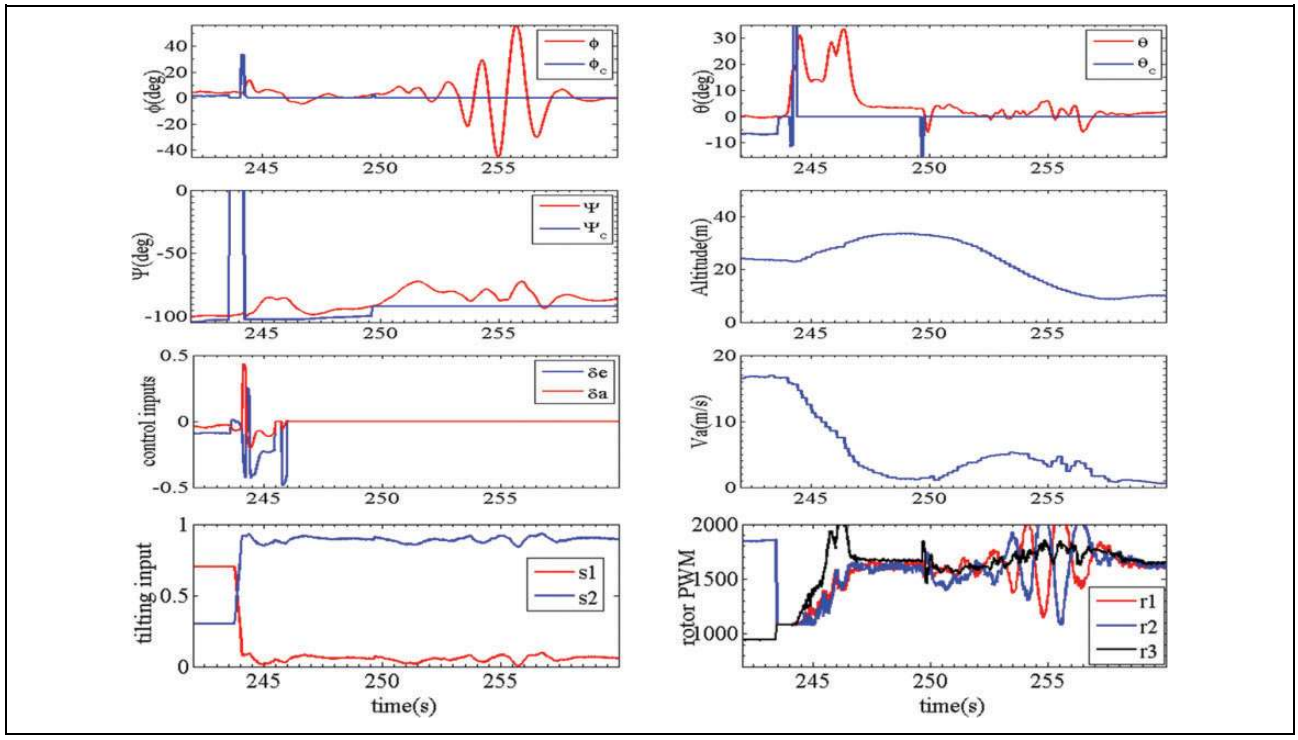

Figure 12. Flight results in rotor and reconversion mode. s1 and s2 represent the servo motors 1 and 2, respectively; r1, r2, and r3 represent rotors 1, 2, and 3, respectively.

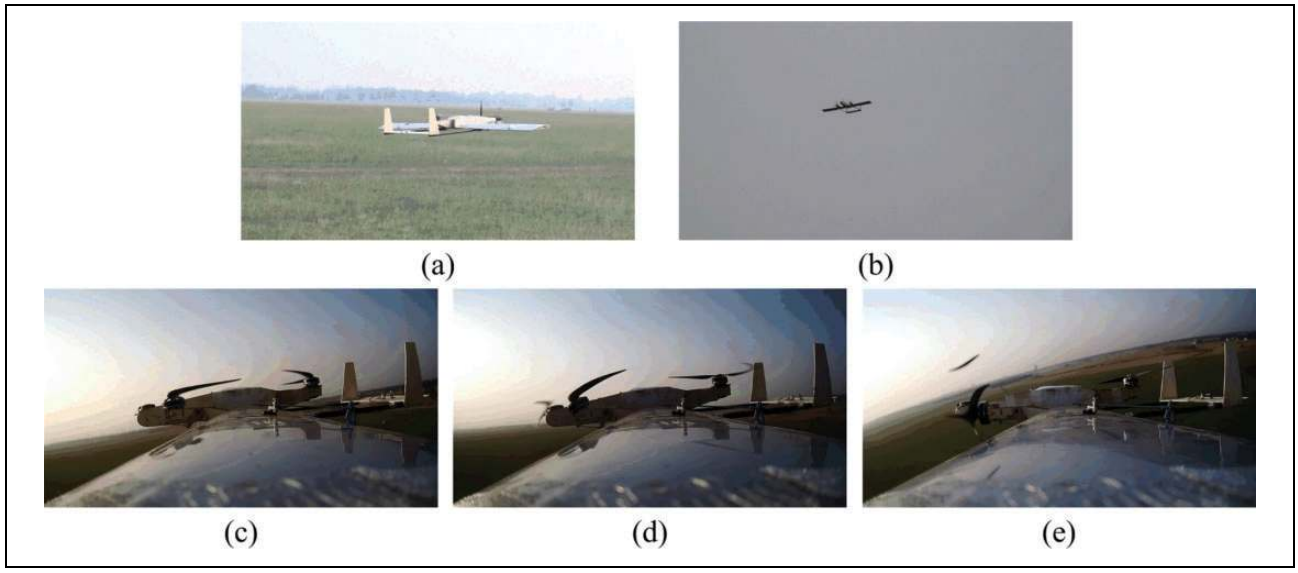

Figure 13. Flight snapshots of the flight.

according to the performance and features of the tilt-rotor UAV, which reduce the cost. Moreover, a control allocation method is proposed to solve the problem that the system is not input-affine and that the number of actuators is different from the number of control channels. The successful autonomous full-mode flight test shows that, regardless of the flight mode, even if there are large deviations of the attitude from the equilibrium state, the tilt-rotor UAV can restore stability and demonstrates that the flight strategy is feasible and the control allocation is effective. Future work will enhance electromagnetic isolation to reduce the effect on the compass, optimize the switching process between rotor and fixed-wing position control to reduce oscillations, install a sensor for the tilting angle, and further increase the flight duration by adopting carbon composite materials to reduce weight.

Declaration of conflicting interests

The author(s) declared no potential conflicts of interest with respect to the research, authorship, and/or publication of this article.

Funding

The author(s) received no financial support for the research, authorship, and/or publication of this article.

References

1. Saeed AS, Younes AB, Islam S, et al. A review on the platform design, dynamic modeling and control of hybrid UAVs. In: *2015 international conference on unmanned aircraft systems (ICUAS)* (ed K Valavanis), Denver, CO, USA, 9–12 June 2015, pp. 806–815. IEEE.
2. The Bell Eagle Eye UAS. http://www.bellhelicopter.com/en/aircraft/military/bellEagleEye.cfm (2008, accessed September 2008).
3. Choi SW, Lee MK, Chang S, et al. Development of practical tiltrotor UAV. In: *50th AIAA aerospace sciences meeting including the new horizons forum and aerospace exposition*, Nashville, Tennessee, 9–12 January 2012, p. 848. American Institute for Aeronautics and Astronautics.
4. Israel Aerospace Industries. http://www.iai.co.il/2013/36944-en/BusinessAreas_UnmannedAirSystems.aspx (2015, accessed March 2016).
5. Firefly6. Birds eye viewofficial website. http://www.birdseyeview.aero/products/firefly6 (2015, accessed December 2015).
6. Carlson S. *A hybrid tricopter/flying-wing VTOL UAV*. Reston: American Institute of Aeronautics and Astronautics, 2014.
7. Yuksek B, Vuruskan A, Ozdemir U, et al. Transition flight modeling of a fixed-wing VTOL UAV. *J Intell Robot Syst* 2016; 84(83): 1–23.
8. Quantum System. http://www.quantum-systems.com/products/tron/ (2015, accessed July 2016).
9. Rysdyk RT and Calise AJ. Adaptive model inversion flight control for tilt-rotor aircraft. *J Guid Control Dyn* 1999; 22(3): 402–407.
10. Kang Y, Kim N, Kim B-S, et al. Autonomous waypoint guidance for tilt-rotor unmanned aerial vehicle that has nacelle-fixed auxiliary wings. *Proc Inst Mech Eng G J Aerosp Eng* 2014; 228(14): 2695–2717.
11. Kim B-M, Choi K, and Kim BS. Trajectory tracking controller design using neural networks for tiltrotor UAV. In: *AIAA guidance, navigation and control conference and exhibit*, Hilton Head, South Carolina, 20–23 August 2007, pp. 20–23. American Institute for Aeronautics and Astronautics.
12. Chowdhury AB, Kulhare A, and Raina G. Back-stepping control strategy for stabilization of a tilt-rotor UAV. In: *2012 24th Chinese control and decision conference (CCDC)* (ed G-H Yang), Taiyuan, China, 23–25 May 2012, pp. 3475–3480. IEEE.
13. Jin K, Xia QY, and Xu JF. Tilt-rotor aircraft modeling and its manipulation assignment strategy. *J Aerosp Power* 2013; 2013: 2016–2028.
14. Kang Y-S, Park B-J, Yoo C-S, et al. Ground test results of rotor governor and rate sas for small tilt rotor UAV. In: *International conference on c*, Seoul, KOREA, 17–20 October 2007, pp. 830–835. Yakdae-Dong: IEEE.
15. Kang Y, Park B, Yoo C, et al. Flight test results of automatic tilt control for small scaled tilt rotor aircraft. In: *International conference on c ICCAS 2008*, Seoul, KOREA, 14–17 October 2008, pp. 47–51. Yakdae-Dong: IEEE.
16. Kang Y, Park B-J, Cho A, et al. Development of flight control system and troubleshooting on flight test of a tilt-rotor unmanned aerial vehicle. *Int J Aeronaut Space Sci* 2016; 17(1): 120–131.
17. Jiandong G. *Flight control of unmanned tiltrotor aircraft*. PhD Thesis. Nanjing University of Aeronautics and Astronautics, China, 2013.
18. Johansen TA and Fossen TI. Control allocation-a survey. *Automatica* 2013; 49(5): 1087–1103.
19. An S-I and Kwon D-S. Robust control allocation of redundantly actuated variable structure systems. In: *International conference on control automation and systems (ICCAS)*, Gyeonggi, KOREA, 27–30 October 2010, pp. 491–496. Yakdae-Dong: IEEE.
20. Francesco GD, D'Amato E, and Mattei M. Incremental nonlinear dynamic inversion and control allocation for a tilt rotor UAV. In: *Guidance navigation and control conference proceedings, AIAA Scitech*, National Harbor, Maryland, 13–17 January 2014. American Institute for Aeronautics and Astronautics.
21. Bodson M. Evaluation of optimization methods for control allocation. *J Guid Control Dyn* 2002; 25(4): 703–711.
22. Härkegård O. Dynamic control allocation using constrained quadratic programming. *J Guid Control Dyn* 2004; 27(6): 1028–1034.
23. 3drobotics Official Website. https://store.3drobotics.com/t/pixhawk/ (2015, accessed December 2015).
24. Qgroundcontrol official website. http://qgroundcontrol.org/ (2015, accessed July 2016).
25. Px4 Official Website. http://dev.px4.io/concept-architecture.html (2015, accessed July 2016).
26. Park S, Deyst J, and How JP. A new nonlinear guidance logic for trajectory tracking. In: *AIAA guidance, navigation, and control conference and exhibit*, 2004, pp. 16–19.
27. Rysdyk R.UAV path following for constant line-of-sight. In: *2th AIAA unmanned unlimited conference and workshop and exhibit*, San Diego, CA, 2003.
28. Mellinger D and Kumar V. Minimum snap trajectory generation and control for quadrotors. In: *2011 IEEE international conference on robotics and automation (ICRA)* (ed L Zexiang), Shanghai, China, 9–13 May 2011, pp. 2520–2525. IEEE.
29. Çetinsoy E, Dikyar S, Hançer C, et al. Design and construction of a novel quad tilt-wing UAV. *Mechatronics* 2012; 22(6): 723–745.